
Imaging Gene Expression in the Brain In Vivo in a Transgenic Mouse Model of Huntington's Disease with an Antisense Radiopharmaceutical and Drug-Targeting Technology

Hwa Jeong Lee, PhD¹; Ruben J. Boado, PhD¹; Dwaine A. Braasch, PhD²; David R. Corey, PhD²; and William M. Pardridge, MD¹

¹Department of Medicine, UCLA School of Medicine, Los Angeles, California; and ²Department of Pharmacology, University of Texas Southwestern Medical Center, Dallas, Texas

Disease-specific genes of unknown function can be imaged in vivo with antisense radiopharmaceuticals, providing the transcellular transport of these molecules is enabled with drug-targeting technology. The current studies describe the production of 16-mer peptide nucleic acid (PNA) that is antisense around the methionine initiation codon of the huntingtin gene of Huntington's disease (HD). **Methods:** The PNA is biotinylated, which allows for rapid capture by a conjugate of streptavidin and the rat 8D3 monoclonal antibody (mAb) to the mouse transferrin receptor (TfR), and contains a tyrosine residue, which enables radiolabeling with ¹²⁵I. The reformulated PNA antisense radiopharmaceutical that is conjugated to the 8D3 mAb is designated ¹²⁵I-PNA/8D3. This form of the PNA is able to access endogenous transferrin transport pathways at both the blood-brain barrier and the brain cell membrane and undergoes both import from the blood to the brain and export from the brain to the blood through the TfR. **Results:** The ability of the PNA to hybridize to the target huntingtin RNA, despite conjugation to the mAb, was shown both with cell-free translation assays and with ribonuclease protection assays. The ¹²⁵I-PNA/8D3 conjugate was administered intravenously to either littermate control mice or to R6/2 transgenic mice, which express the exon 1 of the human HD gene. The mice were sacrificed 6 h later for frozen sectioning of the brain and quantitative autoradiography. The studies showed a 3-fold increase in sequestration of the ¹²⁵I-PNA/8D3 antisense radiopharmaceutical in the brains of the HD transgenic mice in vivo, consistent with the selective expression of the HD exon-1 messenger RNA in these animals. **Conclusion:** These results support the hypothesis that gene expression in vivo can be quantitated with antisense radiopharmaceuticals, providing these molecules are reformulated with drug-targeting technology. Drug targeting enables access of the antisense agent to endogenous transport pathways, which permits passage across the cellular barriers that separate blood and intracellular compartments of target tissues.

Key Words: blood-brain barrier; peptide nucleic acid; transferrin receptor; streptavidin; monoclonal antibody

J Nucl Med 2002; 43:948-956

The availability of the human genome sequence and the emerging applications of functional genomics will lead to the discovery of many novel genes that are expressed in a disease-specific pattern (1). Such novel genes have known sequence but unknown function. For example, the majority of genes uniquely expressed in brain cancer are genes of unknown function (2). The only way to image in vivo a gene of unknown function is with antisense radiopharmaceuticals that hybridize to a specific nucleotide sequence within the target messenger RNA (mRNA) molecule. However, the in vivo applications of antisense radiopharmaceuticals have been limited by the poor transcellular transport and organ distribution of these molecules in living organisms (3). Phosphodiester (PO)-oligodeoxynucleotides (ODNs) are rapidly degraded in vivo by endo- and exonucleases (4). Phosphorothioate (PS)-ODNs are metabolically stable in vivo but are avidly bound by serum proteins (5), retarding uptake into tissues (6). In addition, the highly reactive sulfur atoms in the PS-ODN cause these molecules to nonspecifically bind to many cellular proteins (7), causing nonspecific sequestration of the PS-ODN. A third class of antisense radiopharmaceuticals are peptide nucleic acids (PNAs), which are metabolically stable in vivo and are not bound by serum or tissue proteins. However, PNAs are poorly transported across biologic membranes and must be physically injected into the intracellular space of a cell in tissue culture to hybridize to the target mRNA molecule (8).

The problem of poor transcellular transport of PNA antisense radiopharmaceuticals in vivo is most severe for imaging of transcripts in the brain because of the blood-brain barrier (BBB). The delivery of a PNA from the blood to the intracellular space of the brain cells is a "2-barrier"

Received Sep. 20, 2001; revision accepted Mar. 25, 2002.
For correspondence or reprints contact: Ruben J. Boado, PhD, UCLA Warren Hall (13-164), 900 Veteran Ave., Los Angeles, CA 90024.
E-mail: rboado@mednet.ucla.edu

drug-targeting problem. The PNA must circumvent both the brain capillary endothelial cell, which forms the BBB *in vivo*, and then the brain cell membrane (BCM). Both the BBB and the BCM can be traversed with the introduction of drug-targeting technology (9). In this approach, transcellular transport of the PNA radiopharmaceutical is enabled by conjugation of the PNA to a transport vector. The transport vector is an endogenous peptide or peptidomimetic monoclonal antibody (mAb) that undergoes both receptor-mediated transcytosis across the BBB and receptor-mediated endocytosis across the BCM. The transferrin receptor (TfR) is expressed at both the BBB and the BCM (Fig. 1A), and prior work in rats showed that the murine OX26 mAb against the rat TfR could deliver a PNA radiopharmaceutical to experimental brain tumors *in vivo* (10).

The OX26 mAb used in prior studies in rats does not recognize the murine TfR and is not active in the mouse as a drug-targeting vector (11). Considering the use of transgenic mouse models of neurologic disease, it would be useful to develop technology that would enable the *in vivo* imaging of gene expression in the brain in the mouse using sequence-specific antisense radiopharmaceuticals. In the present studies, the 8D3 rat mAb to the mouse TfR (11) is used as a brain drug-targeting vector to enable imaging of gene expression *in vivo* in a transgenic mouse model of Huntington's disease (HD). The R6/2 transgenic mouse model of HD expresses exon 1 of the huntingtin gene, which contains the expanded CAG repeats characteristic of HD (12). Humans without HD have 6–39 CAG repeats in the huntingtin gene, whereas patients with HD express 36–180 CAG repeats in this gene. The R6/2 transgenic mouse has 1 intact copy of human HD exon 1 that contains 114 CAG repeats, and these mice develop neuronal inclusion bodies and behavioral changes as early as 5 wk after birth (12). The

HD model was developed for antisense imaging of gene expression *in vivo* because prior work showed that sequence-specific antisense agents specifically hybridize to target sequences of the huntingtin mRNA (13).

A PNA that specifically hybridizes to exon 1 of the HD gene was synthesized with a carboxyl terminal tyrosine residue to enable radiolabeling with ^{125}I (Fig. 1B). The amino terminus of the PNA contains an extended biotin group. The biotin moiety allows for rapid capture by streptavidin (SA), which is covalently conjugated through a stable thiol–ether linkage (-S-) to the 8D3 rat mAb to the mouse TfR (Fig. 1B). The use of avidin–biotin technology allows for the high-efficiency coupling of the PNA antisense radiopharmaceutical to the brain drug-targeting vector (Fig. 1B).

MATERIALS AND METHODS

Materials

^{125}I -Na iodine and autoradiographic ^{125}I microscale 20- μm standard strips were purchased from Amersham Pharmacia Biotech (Piscataway, NJ). ^3H -Leucine (6,623 GBq [179 Ci]/mmol) and [^{32}P - α]ATP (29,600 GBq [800 Ci]/mmol) were purchased from Perkin Elmer (Boston, MA). The *m*-maleimidobenzoyl-*N*-hydroxysuccinimide ester and trifluoroacetic acid (TFA) were obtained from Pierce Chemical Co. (Rockford, IL). Acetonitrile (high-performance liquid chromatography grade) was purchased from Fisher Scientific (Pasadena, CA). Recombinant SA, chloramine T, and all other reagents were supplied by Sigma-Aldrich, Inc. (St. Louis, MO). C_{18} Sep-Pak extraction cartridges were obtained from Waters Corp. (Milford, MA). Male BALB/c mice (25–30 g) were purchased from Harlan Sprague-Dawley (San Diego, CA). HD exon-1 transgenic mice (male, 7–8 wk old, 20–25 g [strain name: B6CBA-TgN(HDexon1)62Gpb]), also called R6/2 mice, and littermate control mice were supplied by The Jackson Laboratory (Bar Harbor, ME). T3-TNT translation system, T3

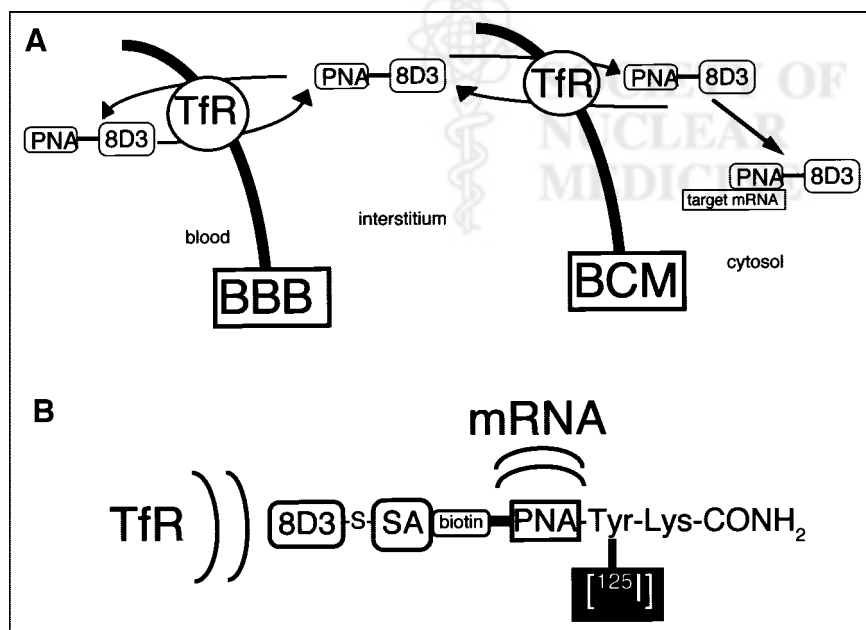


FIGURE 1. (A) "Import-export" model showing bidirectional movement of 8D3 mAb to TfR. Bidirectional movement of PNA-8D3 conjugate across either BBB or BCM is possible because of ability of 8D3 mAb to access endogenous transport pathways for transferrin, which exist at both cellular barriers. Access to TfR pathways allows PNA radiopharmaceutical to move between blood and intracellular compartment of target cell. (B) Conjugation of PNA to 8D3 mAb to TfR creates bifunctional molecule that both accesses TfR for transport between tissue compartments and binds to target mRNA based on sequence specificity of nucleotide residues of PNA radiopharmaceutical. PNA has biotin moiety at amino terminus to allow for capture by conjugate of 8D3 mAb and SA and has carboxyl terminal tyrosine (Tyr) or lysine (Lys) residues to allow for radiolabeling with ^{125}I or ^{111}In , respectively.

RNA polymerase, and EcoRI were obtained from Promega (Madison, WI). Custom ODNs were purchased from Biosource International (Camarillo, CA). Ribonuclease (RNase) T1 was obtained from Invitrogen (San Diego, CA).

Antisense Radiopharmaceutical

The PNA complementary to nucleotides -1 to +15 of the human HD exon 1 is designated HD-PNA (Fig. 2A) and was synthesized at the University of Texas Southwestern Medical Center using automated synthesis described previously (14). The biotin at the amino terminus is followed by 5 linkers (designated -O-), a 16-mer PNA sequence, another 5 linkers, a tyrosine and lysine residue, and an amidated carboxyl terminus. Each of the 5 linkers is composed of 2-aminoethoxy-2-ethoxy acetic acid (Applied Biosystems, Foster City, CA), which is incorporated during the PNA synthesis. The calculated molecular mass of the PNA was 6,316 Da, and the observed molecular mass of the PNA was 6,315 Da as determined by mass spectrometry. A negative control PNA that should not hybridize to the HD transcript was prepared with a sequence antisense to the firefly luc gene as previously described (10). The antiluciferase PNA, designated luc-PNA, was custom synthesized at PE Biosystems (Framingham, MA); had the following nucleic acid sequence: CTTCCATTTTACCAAC; and contained biotin, 5 linkers flanking the nucleotide sequence, tyrosine, and lysine in an order identical to HD-PNA (Fig. 2A).

The targeting vector was composed of a conjugate of recombinant SA and the antimouse TfR mAb (Fig. 1B). Two different rat TfR mAbs were evaluated: the 8D3 mAb and the RI7-217 mAb (11). Initial studies showed the conjugate of SA and the 8D3 mAb, designated 8D3-SA, was more active in vivo than the RI7-217-SA conjugate, and subsequent studies were performed only with the 8D3-SA conjugate. Owing to the very high affinity of SA for biotin (15), there was instantaneous capture of the biotinylated PNA on mixing with the 8D3-SA vector to form the imaging agent shown in Figure 1B. The complex of the ¹²⁵I-PNA bound to the 8D3-SA conjugate constitutes the imaging agent used in the transgenic mouse studies and is designated the PNA-8D3 conjugate.

Iodination of PNA

Biotinylated HD-PNA or luc-PNA (1.8 nmol), ¹²⁵I-Na iodine (74–148 MBq [2–4 mCi], 1–2 nmol), and chloramine T (17.7 nmol) were mixed at a total volume of 55 μL of phosphate buffer (pH = 7.4) at room temperature for 1 min. The reaction was stopped by adding sodium metabisulfite (62 nmol) and then added to either a C₁₈ Sep-Pak extraction cartridge or to a Sephadex G-25 gel filtration column (Amersham Biosciences, Piscataway, NJ). The Sep-Pak cartridge was washed with 10 mL of 0.1% TFA and 5 mL of 5% acetonitrile containing 0.1% TFA, and the ¹²⁵I-HD-PNA was eluted with 5 mL of 40% acetonitrile per 0.1% TFA and was stored at 4°C after evaporation of acetonitrile using a Speed Vac Concentrator (Savant Instrument, Inc., Holbrook, NY). Before application, the 0.7 × 28 cm column of Sephadex G-25 was preequilibrated with 0.01 mol/L Na₂HPO₄, 0.15 mol/L NaCl (pH = 7.4), and 0.05% Tween-20 (ICI Americas Inc., Bridgewater, NY) (PBST), and the sample was eluted with PBST. The final specific activity of the ¹²⁵I-HD-PNA was 2,331–4,440 kBq (63–120 μCi)/μg with a trichloroacetic acid (TCA) precipitability of >96%.

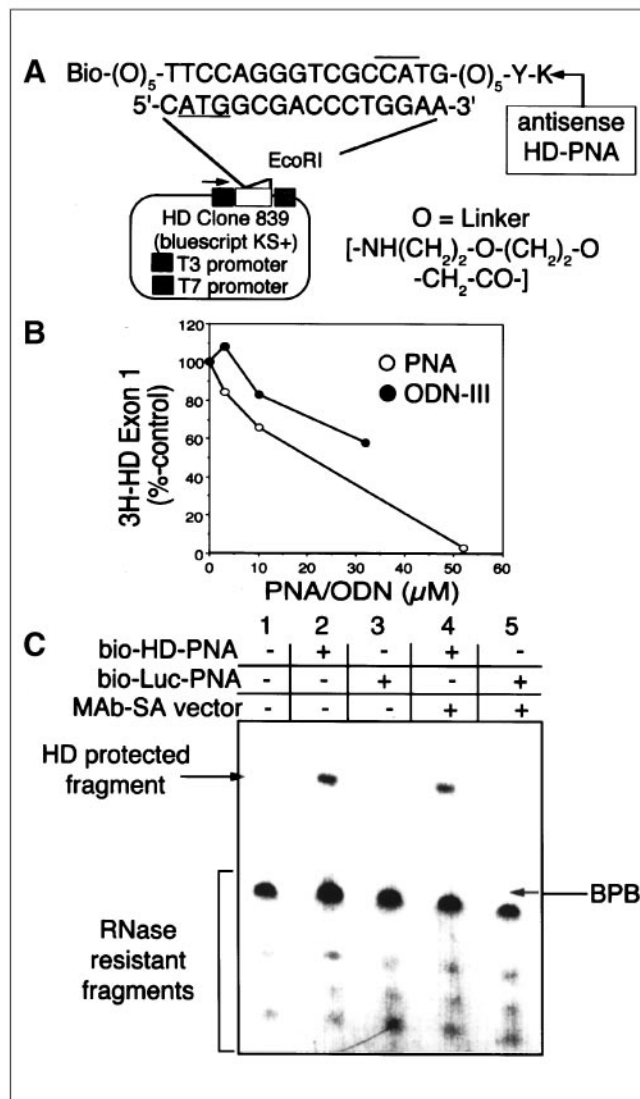


FIGURE 2. (A) Nucleotide sequence (in 5' to 3' orientation) of HD-PNA is bordered on amino terminus by biotin (bio) residue and by tyrosine (Y) and lysine (K) residues at carboxyl terminus. There are 5 linkers (designated O) flanking nucleotide sequence. Complementary nucleotide sequence of HD target mRNA (in 5' to 3' orientation) is shown, and methionine initiation codon (ATG) is underlined. HD exon-1 sequence is downstream of T3 RNA polymerase promoter (left solid box denoted by arrow), which allows for in vitro transcription of HD exon-1 mRNA. (B) Combined in vitro transcription/translation assays resulted in formation of ³H-labeled exon-1 huntingtin protein that was precipitated by TCA. Translation of HD exon-1 protein was inhibited in dose response by either PO-ODN (III) or by PNA. (C) RNase protection assay shows formation of HD mRNA protected fragment after complete nuclease digestion, because of hybridization of biotinylated HD PNA to huntingtin exon-1 mRNA (lane 2). Conjugation of antisense PNA to mAb-SA transport vector does not inhibit the hybridization of PNA to target mRNA, based on formation of RNase protected oligonucleotide shown in lane 4. Conversely, no protected fragment is observed after mixing of anti-luc PNA with HD RNA, either in unconjugated form (lane 3) or conjugated to mAb-SA vector (lane 5). BPB = bromophenol blue.

In Vivo Pharmacokinetics and Organ Uptake in BALB/c Mice

Adult male BALB/c mice were divided into 5 groups of 3 mice each for the pharmacokinetic study. The mice were anesthetized with an intraperitoneal injection of ketamine hydrochloride (100 mg/kg) and xylazine hydrochloride (2 mg/kg). The injection solution contained 185 kBq (5 μ Ci) of [125 I]-HD-PNA with or without conjugation to 2 μ g of 8D3-SA in 0.01 mol/L PBS (pH = 7.4), and a total volume of 50 μ L was administered through the jugular vein of each mouse. Groups of 3 mice each were killed at 0.25, 2, 5, 15, and 60 min after the isotope injection and arterial blood was sampled from the aorta. After spinning the blood samples, the collected supernatant (serum) was counted for 125 I radioactivity using a γ -counter (Beckman Instruments, Inc., Fullerton, CA). An aliquot of serum was precipitated with cold 10% TCA, and the fraction of total serum radioactivity that was TCA precipitated was determined. The brain and peripheral organs (liver, kidney, heart, lung, and spleen) were removed from each mouse at 60 min after the isotope administration, and total 125 I radioactivity in the organ was measured.

For the brain efflux study, BALB/c mice were divided into 4 groups of 3 mice each and 50 μ L of phosphate-buffered saline (PBS) (pH = 7.4) containing 185 kBq (5 μ Ci) of 125 I-HD-PNA with or without 3.2 μ g of 8D3-SA conjugate were intravenously injected into the anesthetized mice. Blood was withdrawn from the aorta, and the 4 groups of 3 mice each were decapitated to remove the brain at 1, 2, 4, and 6 h after injection.

Pharmacokinetic parameters were determined by fitting the serum TCA-precipitable radioactivity data to a biexponential equation with a weighting factor of $[1/A(t)]^2$ using a derivative-free nonlinear regression analysis (PARBMDP, Biomedical Computer P-Series; UCLA Health Science Computing Facilities):

$$A(t) = A_1 e^{-k_1 \cdot t} + A_2 e^{-k_2 \cdot t},$$

where $A(t)$ = % injected dose (%ID)/mL serum at a given time (t).

The organ permeability–surface area (PS) product of either the unconjugated 125 I-HD-PNA, or the 125 I-HD-PNA conjugated to 8D3-SA, was calculated as follows:

$$PS = \frac{[V_d - V_0] \cdot C_p(t)}{AUC_0^t},$$

where $C_p(t)$ is the terminal serum concentration (%ID/mL), AUC is the area under the serum concentration curve from time 0 to the terminal time (t), V_d is the organ volume of distribution, and V_0 is the organ plasma volume, as reported previously (11). The V_d of 125 I-HD-PNA or 125 I-HD-PNA conjugate was calculated from the ratio of counts per minute (cpm) per gram of organ divided by cpm/ μ L of serum at the terminal time (t) after injection.

The brain delivery of the compound was expressed as %ID/g brain and was calculated as follows:

$$\%ID/g = [V_d - V_0] \cdot C_p(t).$$

Quantitative Autoradiography

HD R6/2 transgenic mice and littermate control mice were injected with 150 μ L of PBST through the jugular vein under ketamine hydrochloride and xylazine hydrochloride anesthesia, as described above. The injection solution contained 1,850 kBq (50 μ Ci) of (a) unconjugated 125 I-HD-PNA, (b) 125 I-HD-PNA conju-

gated to 20 μ g of 8D3-SA (1:1 molar ratio), or (c) 125 I-luc-PNA conjugated to 20 μ g of 8D3-SA. The animals recovered from anesthesia within 60 min and were reanesthetized and killed 6 h after the isotope administration. The brain of each mouse was rapidly removed, cut into sagittal slabs, immediately frozen in powdered dry ice, and dipped in Tissue-Tek optimal-cutting-temperature embedding compound (Sakura Finetek, Inc., Torrance, CA). Cryostat sections of frozen brain blocks of 20- μ m thickness were prepared on a Mikrome 505HE cryostat (Micon Instruments, Inc., San Diego, CA), mounted on glass slides, and dried at room temperature.

For film autoradiography, the sections were exposed with intensifying screens to either Biomax MS film (Kodak, Rochester, NY) for 5 d or Kodak X-Omat Blue XB-1 film for 7 d at -70°C in parallel with 20- μ m autoradiographic 125 I microscale standard strips. The films were then developed for 0.5 min using Kodak developer and fixed for 5 min using Kodak fixer. The films were scanned in a 1200 dpi PowerLookIII scanner (Umax Data Systems, Hsinchu, Taiwan) with transparency adapter and cropped in Photoshop 5.5 (Adobe Systems, Inc., San Jose, CA) on a G4 Power Macintosh (Apple Computer, Inc., Cupertino, CA). The integrated density over either the whole-brain section or the 125 I microscale standard was quantified using Image 1.62 software (National Institutes of Health, Bethesda, MD) and normalized by pixel area of the scanned region. The standard curve constructed from 125 I microscale standards was used to convert the integrated density to brain radioactivity normalized by organ weight (kBq [μ Ci]/g).

Translation Arrest

The hybridization of the antisense HD-PNA to the HD transcript was determined using a combination of transcription and translation that mimics *in vivo* conditions as previously described (13). The cDNA containing the human HD exon 1 was subcloned into the Bluescript KS+ plasmid (Stratagene, San Diego, CA), between either T3 or T7 RNA polymerase promoters, and this plasmid is designated clone 839, as described previously (13). Transcription and translation of human HD exon-1 clone 839 was performed with 0.2 μ g clone 839 plasmid DNA in the presence of T3 RNA polymerase, 185 kBq ^3H -leucine, and 50% v/v rabbit reticulocyte lysate using the T3-TNT translation system (Promega, Madison, WI), as described previously (13). Dose response studies with newly synthesized PNAs were performed and compared with a positive control antisense phosphodiester-ODN, designated ODN-III, as previously described (13). Samples were incubated for 30 min at 30°C , and incorporation of ^3H -leucine into HD exon 1 protein was analyzed by trichloroacetic acid (TCA) precipitation, and data expressed as percentage of control, which lacked any added PNA or ODN. The HD exon-1 insert is 10% of the total plasmid, or approximately 0.03 μ g per 12.5 μ L reaction. Since the TNT produces 10–30 RNA copies per plasmid, the final concentration of the HD RNA in the TNT reaction is approximately 1 μM . Therefore, concentrations of 5–50 μM antisense PNA or PO-ODN were used in the TNT assay.

RNase Protection Assay

The HD RNase protection assay (RPA) was used to show specific hybridization of the anti-HD PNA to the target HD mRNA despite conjugation of the PNA to the Tfr mAb-SA vector, as described previously (16). The sense RNA was synthesized with T3 RNA polymerase after linearization of the plasmid with EcoRI. The transcribed RNA was radiolabeled with [^{32}P - α]ATP to a

specific activity of 8.14 kBq [0.22 μ Ci]/pmol, as previously described (17). For the RNase protection assay, 0.6 pmol of biotinylated HD-PNA or biotinylated luc-PNA, with or without conjugation to 6.4 pmol of mAb-SA, was added to 10^5 cpm of 32 P-labeled sense HD RNA (0.2 pmol) in 3 μ L buffer (80 mmol/L NaCl; 7 mmol/L phosphate buffer; pH = 7.5; 0.1% bovine serum albumin [BSA]), and annealed for 30 min at 42°C. Then 20 units RNase T1 and 2.5 μ g RNase A were added to the samples in 17 μ L of RNase digestion buffer (0.3 mol/L NaCl; 10 mmol/L TRIS; pH = 7.5; 4 mmol/L ethylenediaminetetraacetic acid; 0.02% tRNA; 0.02% BSA) and incubated for 30 min at 37°C. RNA fragments were analyzed with 7 mol/L urea in a 20% polyacrylamide gel electrophoresis after autoradiography, as described previously (16). Labeled RNA and PNAs were heat denatured for 2 min at 95°C and then incubated on ice for 2 min immediately before the experiment or conjugation to mAb-SA.

RESULTS

The hybridization of the HD-PNA to the HD mRNA is sequence specific (Fig. 2A) and was confirmed with both the transcription/translation assay (Fig. 2B) and the RPA (Fig. 2C). The PNA inhibits the cell-free translation of the exon-1 fragment of the HD mRNA in a dose response that is comparable with the dose response inhibition of translation caused by a PO-ODN of the same sequence, and designated PO-ODN-III (Fig. 2B). The hybridization of the PNA to the target HD transcript was verified with the RPA as shown in Figure 2C (lane 2). The RPA was performed with either the unconjugated PNA (lane 2), which has a molecular weight of 6,300 Da, or the PNA conjugated to the mAb-SA vector (lane 4), which has a molecular weight of 200,000 Da. The presence of a PNA-protected RNA fragment after complete nuclease digestion of the HD mRNA is indicative of sequence-specific hybridization of the PNA to the target mRNA molecule. The RPA studies in Figure 2C show that the biotinylated HD PNA specifically hybridizes to the target mRNA, and this hybridization is not altered after conjugation of the PNA to the mAb-SA vector. Conversely, mixing of an anti-luc PNA with the HD RNA did not protect the RNA from nuclease digestion, either in the unconjugated form (lane 3) or as a conjugate with the mAb-SA vector (lane 5).

Before the imaging studies in transgenic mice, the pharmacokinetics and organ uptake of the HD-PNA were examined in control BALB/c mice for both the unconjugated PNA and the PNA conjugated to 8D3-SA. Blood was sampled from the mice over a 60-min period after an intravenous injection of either the free or conjugated 125 I-PNA. The pharmacokinetic parameters are shown in Table 1. The organ uptake of either the unconjugated PNA or the PNA-8D3 conjugate was assayed at 60 min after an intravenous injection of the radiopharmaceutical. The unconjugated PNA was cleared from the plasma at a rate of 9.7 ± 1.3 mL/min/kg (Table 1), and the principal organ responsible for clearance of the unconjugated PNA was the kidney (Table 2). Conjugation of the PNA to the 8D3 mAb resulted in a nearly 5-fold decrease in the plasma clearance of the

TABLE 1
Pharmacokinetic Parameters

Parameter	Unit	125 I-HD-PNA/8D3	125 I-HD-PNA
A ₁	%ID/mL	35 \pm 2	32 \pm 2
A ₂	%ID/mL	20 \pm 1	6.3 \pm 0.7
K ₁	1/min	0.49 \pm 0.04	0.37 \pm 0.04
K ₂	1/min	0.0102 \pm 0.0008	0.0206 \pm 0.0014
t _{1/2} ¹	min	1.4 \pm 0.1	1.9 \pm 0.2
t _{1/2} ²	min	68 \pm 5	34 \pm 3
AUC (60 min)	%ID·min/mL	970 \pm 47	308 \pm 36
AUC (∞)	%ID·min/mL	2,048 \pm 165	399 \pm 49
V _{ss}	mL/kg	176 \pm 8	374 \pm 42
CL	mL/min/kg	1.9 \pm 0.1	9.7 \pm 1.3

Data are mean \pm SE computed by nonlinear regression analysis of serum radioactivity measured at 0.25, 2, 5, 15, and 60 min after intravenous injection of either unconjugated 125 I-HD-PNA or 125 I-HD-PNA/8D3 conjugate. Total of 30 mice were used to generate plasma profiles for either form of PNA. ID = injected dose.

radiopharmaceutical (Table 1) because of a >60% reduction in the renal clearance of the PNA (Table 2). The molecular weight of the PNA-8D3 conjugate, 206,000 Da, is 21-fold greater than the molecular weight of the unconjugated PNA (Methods), and the large size of the PNA-8D3 conjugate eliminates glomerular filtration of the PNA. There was minimal uptake of the unconjugated PNA by the liver, heart, lung, or spleen (Table 2), but the organ uptake of the PNA by TfR-rich organs such as the liver or spleen was increased 30- to 100-fold by conjugation to the 8D3 mAb (Table 2). The organ uptake of the 125 I-HD-PNA-8D3-SA conjugate in the transgenic mice was comparable with the organ uptake in the BALB/c mice (Table 2).

The metabolic stability of the HD-PNA was enhanced after conjugation to the 8D3 mAb, based on measurements of serum radioactivity that was precipitated by TCA. For the unconjugated 125 I-PNA, the serum TCA precipitation was 91% \pm 1%, 87% \pm 2%, and 69% \pm 2%, at 5, 15, and 60 min after injection, respectively. For the 125 I-PNA-8D3 conjugate, the serum TCA precipitation was 96% \pm 1%, 97% \pm 1%, 93% \pm 1%, 84% \pm 1%, and 80% \pm 3%, at 5, 15, 60, 120, and 360 min after injection, respectively.

The brain uptake of the unconjugated HD-PNA or the HD-PNA-8D3 conjugate is shown in Figure 3. The BBB PS product of the unconjugated PNA was negligible, <0.3 μ L/min/g, (Fig. 3), which is a very low level of BBB permeability, and comparable with the BBB PS product of sucrose (18), a small molecule that undergoes minimal transport across the BBB in vivo. In contrast, the BBB PS product for the PNA-8D3 conjugate was 1 μ L/min/g, which approximates the BBB PS product for the unconjugated 8D3 mAb in control mice (11). Conjugation of the PNA to the 8D3-SA results in a 3-fold increase in the 60-min plasma AUC (Table 1). Owing to the combined increase in both the BBB PS product and the plasma AUC after conjugation of the PNA to the 8D3-SA, there is a >10-fold

TABLE 2

Organ Uptake of Unconjugated HD-PNA or HD-PNA/8D3 Conjugate at 60 Minutes After Intravenous Administration in Either BALB/c or R6/2 Mice

Organ	BALB/c		R6/2
	¹²⁵ I-HD-PNA	¹²⁵ I-HD-PNA/8D3	¹²⁵ I-HD-PNA/8D3
Liver	0.96 ± 0.02	29 ± 2	40 ± 2
Kidney	36 ± 5	14 ± 1	10 ± 3
Heart	0.56 ± 0.05	1.2 ± 0.1	2.1 ± 0.1
Lung	2.1 ± 0.3	7.0 ± 0.7	8.6 ± 0.1
Spleen	0.64 ± 0.09	80 ± 4	67 ± 5
Thyroid			1.2 ± 0.4
Stomach			2.5 ± 0.1

Data are mean (±SE) %ID/g (n = 3 mice).

increase in the brain uptake of the PNA at 60 min after intravenous injection, when expressed as %ID/g (Fig. 3). The uptake of the PNA-8D3 conjugate by the mouse brain approximated 1 %ID/g (Fig. 3), which is a level of brain uptake of radioactivity that should yield a measurable signal with the in vivo neuroimaging studies in the transgenic mice.

The neuroimaging of gene expression in vivo with a PNA radiopharmaceutical requires imaging the brain at the appropriate time that yields an acceptable signal-to-noise ratio. The signal is derived from hybridization of the PNA to the target mRNA, and the noise is generated from residual unbound PNA in the brain that has not yet effluxed back to the blood. Therefore, after the “import” of the antisense radiopharmaceutical into the brain from the blood, there must be an “export” of the antisense radiopharmaceutical back to the blood from regions of the brain in which there is no specific hybridization of the PNA to the target mRNA. Before in vivo imaging in the transgenic mice, the export of the PNA-8D3 conjugate from the control mouse brain was examined over a 6-h period. In these studies the PNA-8D3

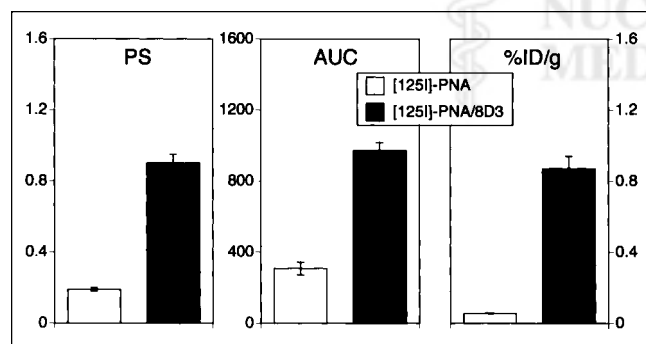


FIGURE 3. BBB permeability–surface area (PS) product, AUC, and brain uptake, expressed as %ID/g brain, is shown for either unconjugated ¹²⁵I-HD-PNA or ¹²⁵I-HD-PNA-8D3 conjugate. Data are mean ± SE (n = 3 mice per group). Units of PS product are μL/min/g and units of 60-min plasma AUC are %ID·min/mL.

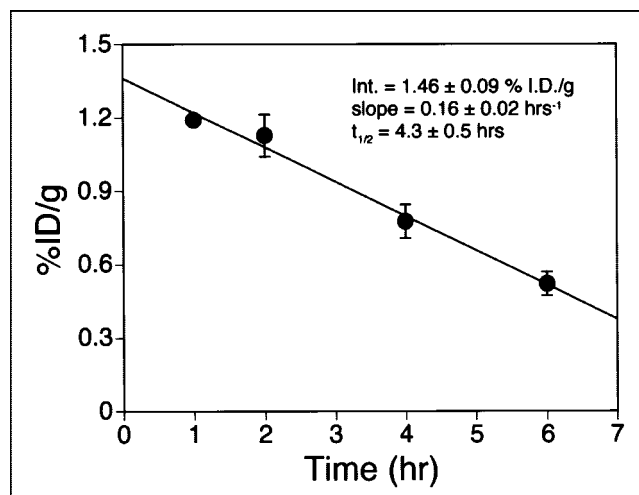


FIGURE 4. Brain uptake, expressed as %ID/g brain, at 1, 2, 4, and 6 h after intravenous injection of ¹²⁵I-HD-PNA-8D3 conjugate is shown. Data are mean ± SE (n = 3 mice per group). Linear regression analysis yielded intercept (Int.) and slope values that are shown. PNA-8D3 conjugate underwent export from brain back to blood with t_{1/2} of 4.3 ± 0.5 h.

radiopharmaceutical was administered intravenously, mice were sacrificed at 1, 2, 4, and 6 h after administration, and brain radioactivity was measured. As shown in Figure 4, there is a monoexponential decay in brain radioactivity after the initial import of the HD-PNA-8D3 conjugate into the mouse brain. The radioactive conjugate effluxes from the mouse brain with a t_{1/2} of 4.3 ± 0.5 h. Therefore, at 6 h after intravenous injection, more than two thirds of the radioactivity initially imported into the brain has effluxed back to the blood. On the basis of these studies, subsequent neuroimaging in the transgenic mice was performed at 6 h after intravenous injection of either the HD-PNA-8D3 conjugate or the luc-PNA-8D3 conjugate.

The brain radioactivity of the HD-PNA-8D3 conjugate at 6 h after intravenous injection is shown for 3 littermate control mice and 3 HD transgenic mice in Figure 5A. These brain scans were quantitated with the ¹²⁵I microscale standard strips (Fig. 5C), and the results of the quantitation are shown in panel D of Figure 5. There is a 3-fold increase in the amount of radioactivity sequestered in the brains of the HD transgenic mice 6 h after intravenous injection as compared with that of the littermate control mice (Fig. 5D). The increase in brain radioactivity in the transgenic mice, as compared with that in the littermate control mice, is also shown by the brain scans (Fig. 5A). In a separate study, additional transgenic mice were examined at 6 h after intravenous injection of either the ¹²⁵I-HD-PNA-8D3 conjugate or the ¹²⁵I-luc-PNA-8D3 conjugate (Fig. 5B). These results show a selective sequestration of the sequence-specific HD-PNA in the brains of the transgenic mice, relative to the brain uptake in the transgenic mice of a control PNA, the luc-PNA (Fig. 5B).

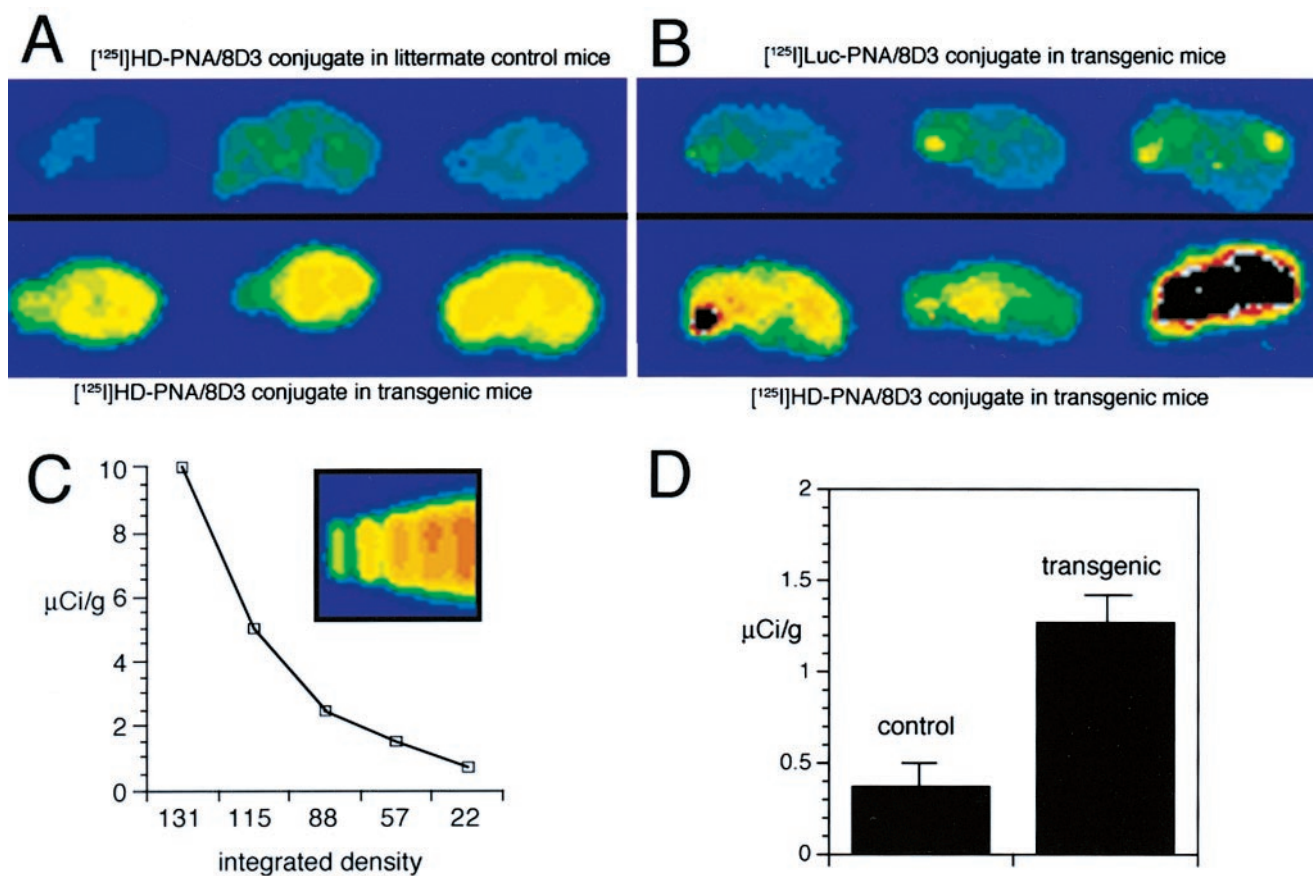


FIGURE 5. (A) Quantitative autoradiography (QAR) of 20- μm frozen sections of brain taken from 3 littermate control mice (top row) or 3 transgenic mice (bottom row) that were killed 6 h after single intravenous injection of ^{125}I -HD-PNA-8D3 conjugate. (B) Film autoradiography of 20- μm frozen sections of brain taken from 3 transgenic mice that were killed 6 h after single intravenous injection of ^{125}I -HD-PNA-8D3 conjugate (bottom row), and 3 transgenic mice that were killed 6 h after single intravenous injection of ^{125}I -luc-PNA-8D3 conjugate (top row). (C) QAR of 20- μm -thick ^{125}I -microscale standard strips is shown in inset. Integrated density for each standard is plotted versus known radioactivity for standard. (D) Integrated density obtained from scanning autoradiograms of brain sections taken from either littermate control mice or transgenic mice (A) was converted into measurements of organ radioactivity (mBq [μCi]/g) based on standard curve (C). Data indicate there is more than 3-fold increase in sequestration of brain radioactivity at 6 h after intravenous injection in transgenic mice compared with littermate control mice. Data are mean \pm SE, $n = 3$ mice per group.

DISCUSSION

The results of these studies are consistent with the following conclusions. First, the pharmacokinetics and organ uptake of a PNA antisense radiopharmaceutical are profoundly altered by conjugation of the PNA to the mAb targeting vector (Tables 1 and 2). Second, the brain uptake of the PNA radiopharmaceutical by the mouse brain is increased by conjugation to the targeting vector, whereas there is no significant uptake of the unconjugated PNA by the mouse brain (Fig. 3). Third, the conjugation of the PNA to the targeting vector enables both the import of the PNA into the brain (Fig. 3) and the export of the PNA-mAb conjugate back to the blood over a 6-h period (Fig. 4). Fourth, conjugation of the PNA to the targeting vector does not affect hybridization of the PNA to the target HD mRNA, based on either cell-free translation or RNase protection assays (Fig. 2). Fifth, the expression of the HD exon-1 gene

in the R6/2 HD transgenic mouse can be detected in vivo with the combined use of a sequence-specific PNA radiopharmaceutical and brain drug-targeting technology. The brain uptake of the ^{125}I -HD-PNA-8D3 conjugate is increased in the transgenic mice compared with littermate controls (Fig. 5A), and the brain uptake of the ^{125}I -HD-PNA-8D3 conjugate in the transgenic mice is increased compared with the brain uptake in these mice of a control luc-PNA-8D3 conjugate (Fig. 5B).

The conjugation of the 6,300-Da PNA to the 200,000-Da mAb-SA targeting system results in an increase in the effective molecular size of the imaging agent. This increase in size decreases systemic clearance 5-fold (Table 1) and blocks glomerular filtration and renal clearance of the PNA (Table 2). Conjugation of the PNA to the targeting vector redirects the antisense agent from kidney to TfR-rich organs such as the liver and spleen (Table 2) or the brain (Fig. 3).

The modest increase in PNA uptake in lung after conjugation to the TfR mAb is consistent with previous studies showing a modest uptake of TfR-specific antibodies in this organ (11). There is little increase in uptake of the PNA by myocardium after conjugation to the targeting mAb (Table 2), as this organ is not targeted by TfR mAbs (11). The conjugation of the PNA to the targeting mAb results in an increase in both the BBB PS product and the plasma AUC, and both contribute to the >10-fold increase in brain uptake of the PNA after conjugation to the 8D3 mAb (Fig. 3). In contrast, the brain uptake of the unconjugated PNA is at the background level consistent with the absence of significant BBB transport of unconjugated PNAs across the BBB in vivo (16). Tyler et al. (19) report that unconjugated PNAs do cross the BBB. However, a quantitative analysis of this study shows that the brain uptake of the unconjugated PNA is <0.0001 %ID/g (19), which is >1,000-fold lower than the brain uptake of the PNA-8D3 conjugate (Fig. 3). Given such a low level of brain uptake of the unconjugated PNA, it would not be possible to measure hybridization of a PNA radiopharmaceutical to a brain-specific target mRNA in vivo after the intravenous administration of an unconjugated PNA.

To image target mRNA molecules in the brain with antisense radiopharmaceuticals, the antisense agent must be able to access transport pathways within the organ that mediate both the import and the export of the antisense agent between the blood and organ compartments. No target mRNA can be imaged if there is no initial import from the blood of the antisense radiopharmaceutical into the target organ. However, there must also be subsequent export of the antisense radiopharmaceutical back to the blood from areas outside the region of interest (ROI) so as to generate a quantifiable image over the ROI. The application of the import-export model with respect to imaging the brain with targeted peptide radiopharmaceuticals has been shown recently in an Alzheimer's disease transgenic mouse model (20). The BBB TfR is a bidirectional transport system (21) and enables the receptor-mediated transcytosis of either transferrin (Tf) or a TfR mAb from the blood to the brain (22). In addition, the BBB TfR also mediates the reverse transcytosis of either Tf or TfR mAbs from the brain back to the blood (21), as shown in Figure 1A. The endogenous transport pathways for Tf at both the BBB and the BCM allow for the sequential import of holo-Tf from the blood to the brain followed by the export of apo-Tf from the brain back to the blood (21). The TfR mAb traces these endogenous Tf transport pathways without interference in the transport of the endogenous Tf (22). By 6 h after intravenous injection of the PNA-8D3 conjugate, there is efflux back to the blood of >67% of the initial radioactivity imported into the brain (Fig. 4). Therefore, subsequent brain scanning in the transgenic mice was performed at 6 h after an intravenous injection of the PNA-8D3 conjugate. Another requisite for in vivo imaging of target mRNA with antisense radiopharmaceuticals is that the hybridization of

the PNA to the target mRNA is not sterically inhibited by conjugation of the PNA to the targeting 8D3-SA vector. The in vitro studies showed that conjugation of the PNA to the 8D3 mAb did not impair the ability of the PNA to hybridize to the target HD mRNA, based on either cell-free translation or RNase protection assays (Fig. 2).

A conjugated PNA radiopharmaceutical that was enabled to access both import and export transport pathways between the blood and the brain (Fig. 1A), and which contained a specific-base sequence, might be selectively sequestered in the brain of animals specifically expressing the target mRNA. This hypothesis is confirmed with the in vivo imaging studies performed on the control littermate mice and the HD exon 1 transgenic mice (Fig. 5A). By 6 h after intravenous injection, more than two thirds of the initial radioactivity in the brain has effluxed back to the blood (Fig. 4), which is consistent with the reduced level of brain radioactivity in the littermate control mice at 6 h (Fig. 5D). In contrast, the brain radioactivity at 6 h is approximately 3-fold greater in the HD transgenic mice than in the littermate control mice (Fig. 5D). The brain scans of the transgenic mice show widespread sequestration of the imaging agent by the HD mRNA (Fig. 5A), consistent with the generalized expression of the HD exon-1 transcript in the brains of these transgenic mice (12). The sequestration of the sequence-specific ¹²⁵I-HD-PNA-8D3 conjugate in the brain of the transgenic mice exceeds that of a control luc-PNA-8D3 conjugate (Fig. 5B). Therefore, the sequence specificity of the PNA provides the basis for the selective sequestration of the antisense radiopharmaceutical once this molecule is targeted to intracellular spaces within the brain.

CONCLUSION

These studies provide support for the hypothesis that it is possible to image gene expression in vivo with sequence-specific antisense radiopharmaceuticals, providing the antisense radiopharmaceutical is reformulated using drug-targeting technology (9). The unconjugated PNA antisense radiopharmaceutical is not specifically taken up by the brain (Fig. 3). Therefore, it is not possible to image gene expression in vivo with an antisense radiopharmaceutical that is not able to circumvent the transcellular barriers that exist in vivo between the blood and the target transcript in the intracellular compartments. In contrast, conjugation of the antisense radiopharmaceutical to a targeting mAb allows the antisense agent to access transport pathways for endogenous ligands, such as Tf (Fig. 1A). Transport by the endogenous pathways enables both the import and the export of the radiopharmaceutical between the blood and target organ compartments. The combined use of both import and export transport pathways allows for hybridization to the target mRNA and selective sequestration of the antisense radiopharmaceutical within the ROI. This study also provides the basis for attempts to image the expression of the huntingtin mRNA in HD patients in vivo, which may assist in the

evaluation of neurotherapeutics that are designed to alter the expression of the huntingtin gene in HD.

ACKNOWLEDGMENTS

This study was supported by a grant from the Hereditary Disease Foundation, by National Institutes of Health grant GM60624, and by U.S. Department of Energy grant ER62655.

REFERENCES

1. Lockhart DJ, Winzler EA. Genomics, gene expression and DNA arrays. *Nature*. 2000;405:827–836.
2. Pardridge WM. Antisense radiopharmaceuticals: agents for imaging gene expression. *Drug Discov Today*. 2001;6:104–106.
3. Hnatowich DJ. Antisense and nuclear medicine. *J Nucl Med*. 1999;40:693–703.
4. Tavittian B, Terrazzino S, Kuhnast B, et al. *In vivo* imaging of oligonucleotides with positron emission tomography. *Nat Med*. 1998;4:467–471.
5. Cossum PA, Sasmor H, Dellinger D, et al. Disposition of the ¹⁴C-labeled phosphorothioate oligonucleotide ISIS 2105 after intravenous administration to rats. *J Pharmacol Exp Ther*. 1993;267:1181–1190.
6. Wu D, Boado RJ, Pardridge WM. Pharmacokinetics and blood–brain barrier transport of [³H]-biotinylated phosphorothioate oligodeoxynucleotide conjugated to a vector-mediated drug delivery system. *J Pharmacol Exp Ther*. 1996;276:206–211.
7. Brown D, Kang S-H, Gryaznov SM, et al. Effect of phosphorothioate of oligodeoxynucleotides on specific protein binding. *J Biol Chem*. 1994;269:26801–26805.
8. Hanvey JC, Pfeffer NJ, Bisi JE, et al. Antisense and antigene properties of peptide nucleic acids. *Science*. 1992;258:1481–1486.
9. Pardridge WM. *Brain Drug Targeting: The Future of Brain Drug Development*. Cambridge, UK: Cambridge University Press; 2001.
10. Shi N, Boado RJ, Pardridge WM. Antisense imaging of gene expression in the brain in vivo. *Proc Natl Acad Sci USA*. 2000;97:14709–14714.
11. Lee HJ, Engelhardt B, Lesley J, Bickel U, Pardridge WM. Targeting rat anti-mouse transferrin receptor monoclonal antibodies through the blood–brain barrier. *J Pharmacol Exp Ther*. 2000;292:1048–1052.
12. Kirupa S, Hobbs C, Mangiarini L, et al. Transgenic models of Huntington's disease. *Phil Trans R Soc Lond B Biol Sci*. 1999;354:963–969.
13. Boado RJ, Kazantsev A, Apostol BL, Thompson LM, Pardridge WM. Antisense-mediated downregulation of the human huntingtin gene. *J Pharmacol Exp Ther*. 2000;295:239–243.
14. Mayfield LD, Corey DR. Automated synthesis of peptide nucleic acids and peptide nucleic acid-peptide conjugates. *Anal Biochem*. 1999;268:401–404.
15. Green NM. Avidin. *Adv Prot Chem*. 1975;29:85–133.
16. Pardridge WM, Boado RJ, Kang Y-S. Vector-mediated delivery of a polyamide (“peptide”) nucleic acid analogue through the blood–brain barrier in vivo. *Proc Natl Acad Sci USA*. 1995;92:5592–5596.
17. Boado RJ, Pardridge WM. Complete inactivation of target mRNA by biotinylated antisense oligodeoxynucleotide-avidin conjugates. *Bioconj Chem*. 1994;6:406–410.
18. Samii A, Bickel U, Stroth U, Pardridge WM. Blood–brain barrier transport of neuropeptides: analysis with a metabolically stable dermorphin analogue. *Am J Physiol*. 1994;267:E124–E134.
19. Tyler BM, Jansen K, McCormick DJ, et al. Peptide nucleic acids targeted to the neurotensin receptor and administered i.p. cross the blood–brain barrier and specifically reduce gene expression. *Proc Natl Acad Sci USA*. 1999;96:7053–7058.
20. Lee HJ, Zhang Y, Zhu C, Duff K, Pardridge WM. Imaging brain amyloid of Alzheimer's disease in vivo in transgenic mice with an A β peptide radiopharmaceutical. *J Cereb Blood Flow Metabol*. 2002;22:223–231.
21. Zhang Y, Pardridge WM. Rapid transferrin efflux from brain to blood across the blood–brain barrier. *J Neurochem*. 2001;76:1597–1600.
22. Skarlatos S, Yoshikawa T, Pardridge WM. Transport of [¹²⁵I] transferrin through the rat blood–brain barrier in vivo. *Brain Res*. 1995;683:164–171.

